LIMNOLOGY and OCEANOGRAPHY

ASLO

Limnol. Oceanogr. 64, 2019, 423–440

doi: 10.1002/lno.11049

Disentangling limnological processes in the time-frequency domain

Silke R. Schmidt [1,2*] **Gunnar Lischeid,** [2,3] **Thomas Hintze,** [1] **Rita Adrian** [1,4]

[1]Department of Ecosystem Research, Leibniz-Institute of Freshwater Ecology and Inland Fisheries, Berlin, Germany
[2]Institute of Earth and Environmental Sciences, University of Potsdam, Potsdam, Germany
[3]Leibniz Centre for Agricultural Landscape Research, Müncheberg, Germany
[4]Department of Biology, Chemistry and Pharmacy, Freie Universität Berlin, Berlin, Germany

Abstract

State variables in lake ecosystems are subject to processes that act on different time scales. The relative importance of each of these processes changes over time, e.g., due to varying constraints of physical, biological, and biogeochemical processes. Correspondingly, continuous automatic measurements at high temporal resolution often reveal intriguing patterns that can rarely be directly ascribed to single processes. In light of the rather complex interplay of such processes, disentangling them requires more powerful methods than researchers have applied up to this point. For this reason, we tested the potential of wavelet coherence, based on the assumption that different processes result in correlations between different variables, on different time scales and during different time windows across the seasons. The approach was tested on a set of multivariate hourly data measured between the onset of an ice cover and a cyanobacterial summer bloom in the year 2009 in the Müggelsee, a polymictic eutrophic lake. We found that processes such as photosynthesis and respiration, the growth and decay of phytoplankton biomass, dynamics in the CO_2-carbonate system, wind-induced resuspension of particles, and vertical mixing all occasionally served as dominant drivers of the variability in our data. We therefore conclude that high-resolution data and a method capable of analyzing time series in both the time and the frequency domain can help to enhance our understanding of the time scales and processes responsible for the high variability in driver variables and response variables, which in turn can lay the ground for mechanistic analyses.

For a long time, limnologists have sought to understand temporal variability in physical, chemical, or biological state variables and the processes behind such variability. Dynamics in these variables can be caused by changes in the prevailing constraints of dominant limnological processes. For example, the potentially exponential growth of phytoplankton populations may be constrained simultaneously or successively by light availability, the supply of nutrients, and grazing pressure from zooplankton (Sommer et al. 1986, 2012). Calcite precipitation often occurs during spring and summer in productive, carbonate-rich water bodies (when the photosynthetic uptake of carbon dioxide increases pH levels [Heine et al. 2017]), while a decrease in pH can lead to calcite dissolution (Lampert and Sommer 2007). Calcite precipitation can, through coprecipitation of phosphate, limit nutrient availability and therefore also phytoplankton growth (Hamilton et al. 2009). Finally, the replenishment of oxygen in oxygen-depleted lake bottoms is constrained to periods of vertical mixing at high wind speeds (Lampert and Sommer 2007; Read et al. 2011). In this regard, research is now increasingly focusing on episodic events and how, for instance, storms affect a lake ecosystem or certain processes in it (Jennings et al. 2012; Klug et al. 2012; Kasprzak et al. 2017). These examples illustrate that the type of prevailing constraint of a limnological process may change over time, and can happen on different time scales ranging from fractions of seconds ([bio-]chemical reaction rates), from seconds to days (photosynthesis), from minutes to days or weeks (mixing processes), from hours to weeks (population dynamics), and even up to several months (seasonal dynamics) (Reynolds 1990; Behrendt et al. 1993; Hanson et al. 2006). Nevertheless, understanding and identifying the huge intra-annual variability of various state variables, their interactions, and their time scales remains challenging.

Analyzing limnological processes, their time scales, and their constraints requires a high amount of multivariate data, which are increasingly being collected in lakes worldwide (Marcé et al. 2016; Meinson et al. 2016). With automated high-frequency measurements, the temporal resolution has become almost unlimitedly high. Patterns of temporal variability in the measured variables may indicate processes, such as photosynthesis and respiration, as indicated by oxygen concentration and

*Correspondence: silke.schmidt@igb-berlin.de

pH (Hanson et al. 2006). However, the way the variation of a variable, or the covariation of two variables, can pinpoint a process and indicate the state of a lake ecosystem is not always straightforward: Many processes may affect more than one single variable; moreover, a given process may affect each of these variables in a different way, on a different time scale, and during a different time window of the year. The inherent complexity of internal and external forces structuring lake ecosystems adds to that variability. There are now a number of studies that have considered the time scales of temporal variability and have separated, e.g., hourly variability from daily, monthly, seasonal, or yearly variability (Benincà et al. 2011; Adrian et al. 2012; Blauw et al. 2012; Kara et al. 2012; Guadayol et al. 2014; Schmidt et al. 2018). Nevertheless, the benefit of using high-frequency measurements over lower-frequency measurements and the role of different time scales of variability still lack sufficient consideration (Adrian et al. 2012; Coble et al. 2016). This means that methods are required that are able to differentiate among processes, time scales, and particular time windows. Once we have identified the temporal patterns and time scales of covariation, subsequent analytical or modeling steps may allow us to further our understanding of the mechanisms that drive overall temporal variability in lakes.

Wavelet coherence (Torrence and Compo 1998; Grinsted et al. 2004; Cazelles et al. 2008) is a method by which the direction and strength of coherence of two time series across different time scales can be analyzed. While wavelet coherence does not necessarily indicate causality between two time series, robust coherence between two variables over particular time scales and during particular time windows can be indicative of processes that typically affect these two variables synchronously. In contrast to correlation analyses, wavelet coherence differentiates among time scales, as the variability of the coherence between two variables is partitioned into frequencies. These range from twice the measurement resolution up to the entire length of the time span under investigation. Importantly, wavelet coherence can track periods of synchronicity even when they are limited to rather short time spans. As such, analysis of the synchronicity of temporal patterns of different variables on different time scales is a necessary first step in disentangling different processes that occur in parallel.

This study aims to disentangle processes characterized by temporal synchronicities among physical, chemical, and biological variables in the Müggelsee, a eutrophic polymictic lake, using wavelet coherence. We intend to identify the most prominent time scales, ranging from hours to months, that these synchronicities operate on across different seasons and water depths. We then discuss the implications of identified patterns for the state of this lake ecosystem. We base our study on a dataset of automated hourly measurements of water temperature; chlorophyll *a* (Chl *a*), as an indicator for algal biomass; phycocyanin, as a proxy for cyanobacterial biomass; oxygen concentration; pH; turbidity; electrical conductivity, quantifying ionic substances; wind speed, as an important meteorological driver of turbulence in the water column; and manually measured ice development. We selected five examples out of a set of many possible combinations of variables where we expected to find a plausible causal relationship that could indicate ecological processes such as photosynthesis, the growth of phytoplankton biomass, particle resuspension, calcite precipitation, and lake mixing. Robust proof of causality would require more elaborate examinations of each single case, and was beyond the scope of this study. We show how coherence between variables in time-frequency space, as well as coherence of a single variable at different measurement depths, can help to identify processes that occur during distinct time windows and at certain frequencies.

Methods

Study site

The Müggelsee is a shallow (mean depth 4.9 m, maximum depth 7.9 m), polymictic, eutrophic lake in northeastern Germany with a surface area of 7.3 km^2 and a mean retention time of 6–8 weeks (Fig. 1; Köhler et al. 2005). The Spree River flows through the Müggelsee and rapidly mixes with the lake

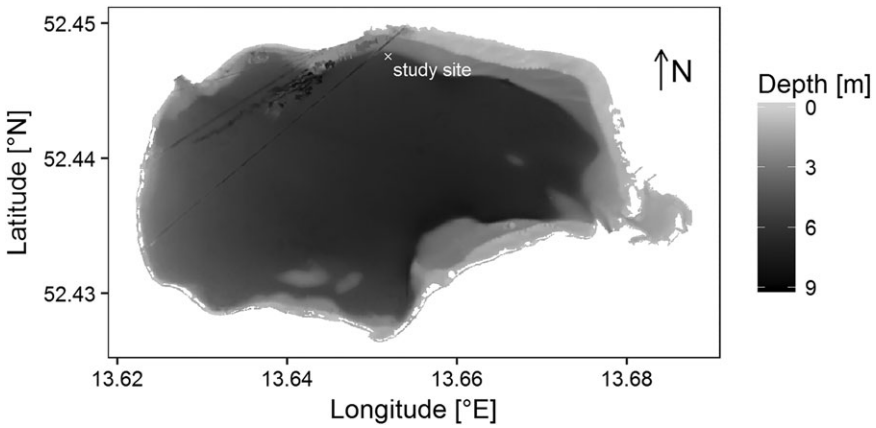

Fig. 1. Bathymetric map of the study site at the Müggelsee in Berlin, Germany.

water (Barthelmes 1962). The Müggelsee is a highly wind-exposed lake. This, together with its shallowness, leads to frequent events of complete mixing that interrupt time windows of thermal stratification (Driescher et al. 1993). Most events of stable thermal stratification during summer are shorter than 1 day, but can occasionally last up to several weeks (Wilhelm and Adrian 2008). The catchment area is 7000 km^2 and is dominated by agriculture and forestry (Driescher et al. 1993). The Müggelsee is a calcium-rich, hard-water lake with high levels of alkalinity (Driescher et al. 1993). The Spree River has a large influence on its water quality (Köhler and Nixdorf 1994), while groundwater withdrawal from wells around the lake reduces any influence of adjacent groundwater on the water quality of the Müggelsee itself. Due to high nutrient levels, the Müggelsee is eutrophic and experiences substantial algal blooms during spring and summer. Summer blooms are often dominated by cyanobacteria (Wagner and Adrian 2009).

Automated sensor measurements

Limnological data were collected by automated measurements with a multiparameter probe (YSI 6600 V2-4) on a platform 300 m from the northern shore of the Müggelsee (52°26′46.1″N; 13°39′00.2″E). The probe measured water temperature, Chl *a*, phycocyanin, turbidity, oxygen, pH, and electrical conductivity at 1.5 m depth below the surface. Water temperature and electrical conductivity were measured with a combined physical sensor. A pH electrode determined hydrogen ion concentrations. Chl *a*, phycocyanin, turbidity, and oxygen were measured with optical sensors, equipped with integrated antifouling wipers for self-cleaning. Once per hour, depth profiles were measured between 0.5 and 5 m depth at increments of 0.5 m. The multiparameter probe has a sampling frequency of twice per second. The hourly time series used for this study are based on the mean of 20 single measurements recorded over a time period of 10 s every hour. The measurements at different depths were performed with an offset of a few minutes. For this reason, we only interpreted time scales exceeding 3 h. During the winter, measurements with the same probe were performed hourly below the ice cover at a fixed depth of 1.5 m at the same location. Therefore, measurements at depths other than 1.5 m were only available after the ice melted in March (the "thaw date"). We used measurements at a depth of 1.5 m to analyze the coherence between different variables, and measurements at depths of 1.5 and 5 m to analyze the coherence of a single variable between these depths. The thickness of the ice cover was measured approximately daily at several locations. Wind speed was measured after the thaw date at the same location of 4 m above the water surface with a cup anemometer (Thies GmbH).

Data preprocessing

We selected a time span between December 2008 and August 2009 that was almost free of data gaps. As the focus of the study was to capture patterns of natural short-term to long-term variability, any kind of gap filling would result in major artifacts. However, even within the selected time span, there were a few short gaps in the dataset. Due to fouling of the optical turbidity sensor, 31 h of turbidity measurements in April were excluded from the analyses. Fouling was indicated by a steep increase of turbidity values before the sensor was cleaned manually. One extreme outlier in Chl *a* measurements in April was excluded as well. Furthermore, there was a gap of 24 h in all variables in March, when the measurement protocol changed from winter measurements to regular measurements that included depth profiles. A 19-h gap in July, a 5-h gap in February, a 2-h gap in August, and four 1-h gaps in June and July occurred due to probe malfunction. All gaps were filled by linear interpolation and are marked in red in all figures. Wavelet coherence, especially at subdaily frequencies, should be interpreted with caution at these instances, as the low variability of the linearly interpolated gaps can lead to spurious results. However, other than the one turbidity measurement gap of 31 h, no gaps were longer than 24 h, and the coherence over longer time scales can therefore be interpreted with sufficient confidence. All variables were normalized to zero mean and unit variance prior to analysis.

Since non-normally distributed time series may lead to unreliable and less statistically significant results of wavelet transforms (Grinsted et al. 2004), and because some of the variables used in our study were not normally distributed, we repeated all analyses on log-transformed data. Most variables exhibited reduced skewness after log-transformation, but only some of them exhibited a normal distribution. We therefore additionally repeated all analyses on the rate of change of the log-transformed data, calculated as the difference between the data values of adjacent time steps. This resulted in normal distributions of all variables. The analyses of original data, log-transformed data, and the rate of change of log-transformed data all resulted in very similar patterns. We therefore only show the results of the original, untransformed data.

Wavelet coherence

We used wavelet coherence (Torrence and Compo 1998; Grinsted et al. 2004; Maraun and Kurths 2004) to detect synchronous fluctuations between two time series. For this purpose, both time series were decomposed via continuous wavelet transform, which transforms time series from the time domain to the time-frequency domain. Wavelet transform is defined as the convolution of a time series x_t with a wavelet ψ_t, i.e., a basis function localized in both time and frequency. We chose the Morlet wavelet as the basis function, because it represents a good compromise between time and frequency resolution, and is commonly used (Torrence and Compo 1998; Cazelles et al. 2008). It is defined as

$$\psi_0(t) = \pi^{-\frac{1}{4}} e^{i\omega_0 t} e^{-\frac{t^2}{2}},$$

where t represents time and ω_0 is the central angular frequency. Continuous wavelet transform at scale f and time τ is given by

$$W(f,\tau) = \frac{1}{\sqrt{f}} \int_{-\infty}^{+\infty} x(t) \psi^* \left(\frac{1-\tau}{f} \right) dt = \int_{-\infty}^{+\infty} x(t) \psi^*_{f,\tau} dt,$$

where $(^*)$ indicates the complex conjugate form (Torrence and Compo 1998, Cazelles et al. 2008). In layman's terms, the wavelet function can be considered a snippet of a sine function, which is subsequently compared to different sections of the time series of observables. In the next step, the frequency of the wavelet function is modified by compressing or extending it along the time axis. This wavelet thus exhibits specific information regarding frequency and time localization. Wavelet coherence is given by the square of the product of the first time series wavelet transform, $W^X_{f,\tau}$, with the complex conjugation of the second, $W^Y_{f,\tau}$, normalized by the individual power spectra of each time series, as

$$R^2_{f,\tau} = \frac{\left| S\left(f^{-1} W^X_{f,\tau} W^{Y*}_{f,\tau} \right) \right|^2}{S\left(f^{-1} \left| W^X_{f,\tau} \right|^2 \right) \cdot S\left(f^{-1} \left| W^Y_{f,\tau} \right|^2 \right)},$$

where S is a smoothing operator in both scale and time (Torrence and Compo 1998; Grinsted et al. 2004; Maraun and Kurths 2004). Wavelet coherence exhibits values between zero and one, and identifies phases of local cross-correlation between two time series as a function of frequency. High values of wavelet coherence can indicate a strong similarity between time series at a particular frequency and during a particular time window. The phase difference between the time series, indicated by arrows in the figures of wavelet coherence, provides information about a possible time lag in the relationships between two variables.

All analyses were performed with R (R Core Team 2018). Wavelet coherence and phase relationships were calculated with the R biwavelet package (Gouhier et al. 2018), whose code is based on the MATLAB's WTC package (Grinsted et al. 2004). We selected a time span long enough to be able to disregard the beginning and end of the time series, and therefore refrained from extending the time series with zeros at the beginning and end (zero padding), as sometimes suggested to reduce edge effects (Torrence and Compo 1998; Vargas et al. 2010). The significance of wavelet coherence was calculated as the significant deviation from red noise, generated by 100 Monte Carlo randomizations of a first-order autoregressive process (AR1) with the same autocorrelation coefficients as the respective input time series. Significance was tested at a significance level of 0.95. Given the massive number of tests performed (all combinations of scale and time; Keitt 2008; Vasseur et al. 2014), we applied a p-value correction (5% level), following Benjamini and Yekutieli (2001). To quantify the intensity of thermal stratification, we calculated the Schmidt stability (Schmidt 1928; Idso 1973) from hourly water temperature profiles using the R rLakeAnalyzer package (Winslow et al. 2016). All figures were created with the R ggplot2 package (Wickham 2009).

In the following, "period length" always refers to the period length in question as 1/frequency. In contrast, references to certain time intervals are termed "time span" if referring to the whole available time interval, or "time window" if shorter periods are meant.

Analyzing patterns for processes

Here, we focus on the following patterns that we related to specific processes. We chose five examples where we expected to find plausible relationships between two variables or between one variable measured at different depths. Some of these patterns are restricted to lakes with circumneutral pH values where hydrogencarbonate (HCO_3^-) is the primary form of dissolved inorganic carbon (Lampert and Sommer 2007), such as in the lake studied here. While some patterns may be identifiable from the data, i.e., cases where the relationship occurs for all time scales, others are restricted to specific time scales that may be masked by lower-frequency variations or blurred by higher-frequency noise. Wavelet coherence is able to disentangle these frequency-dependent patterns.

- Synchronous fluctuations of pH and oxygen (O_2) are ascribed to photosynthesis, where the uptake of CO_2 reduces HCO_3^- concentration and thus increases pH, and the release of O_2 increases oxygen saturation. The opposite pattern holds for respiration. This is likely to occur for all time scales. In contrast, phases of pronounced decay of algal and cyanobacteria biomass will likely only occur at period lengths $\gg$ 1 d.
- A synchronous increase in water temperature, Chl *a* levels, and phycocyanin levels points to a growth in algal and cyanobacteria biomass on a time scale of several hours to days. This can be seen as a measure of the potential photosynthesis of the existent phytoplankton biomass, while synchronous fluctuations of pH and O_2 are related to the actual productivity of the existent phytoplankton biomass.
- Synchronous changes in turbidity and Chl *a* or phycocyanin on time scales $\gg$ 1 d are indicative of a causal relationship between Chl *a* or phycocyanin and turbidity, respectively. In contrast, changes of turbidity that are not reflected by changes in Chl *a* or phycocyanin levels point to, e.g., the input of turbid water via streams during heavy rain storms or sediment resuspension from the bottom layer of the lake, e.g., during heavy wind storms.
- A decrease in electrical conductivity in parallel with an increase in pH points to calcite precipitation, and the

opposite pattern to calcite dissolution. This process is not restricted to specific time scales.

- Changes of single variables at different depths that occur with a reversed sign (indicating a phase shift of half a period length) can be interpreted as an indicator of mixing of shallow and deep water. This phenomenon will likely affect multiple variables in parallel, but might not necessarily be visible for all of them, because not all variables may exhibit a clear depth gradient during that phase. Mixing is not restricted to specific time scales.

Results

The lake was covered with ice from 31 December 2008 until 9 March 2009 (Fig. 2). A phytoplankton bloom had already started underneath the ice and lasted until the onset of the clear water phase around 02 May 2009. In June, the weather was mostly stormy, as indicated by low air pressure, high wind speeds, frequent precipitation, cool air and water temperature, and low Schmidt stability, i.e., favoring mixing (Fig. 2). In July, the weather was more settled, and a stable thermal stratification developed in the lake, as indicated by relatively high Schmidt stabilities (Fig. 2), followed by a cyanobacteria bloom.

Wavelet coherence between two time series is depicted in Figs. 3–11. The time domain is shown on the *x*-axis with the same scaling as for the time series given above, while the respective period length is given on the *y*-axis. Colors indicate the degree of coherence. For example, a red area in the time-frequency space bordered by a black line would mark a range of period lengths and a time window during which two variables fluctuate in a highly coherent way and significantly differ from red noise. The black arrows indicate the phase relationship between two variables at the indicated period length and time window. Arrows pointing right mean that the two variables are in phase, i.e., they oscillate synchronously at that period length. Arrows pointing left mean that synchronicity is in antiphase, hence indicating a phase shift of half a period length; therefore, an increase in one variable is accompanied by a decrease in the other variable, and vice versa. Arrows pointing upwards mean the variables are out of phase with the lead of the first variable, while arrows pointing downward reflect an out-of-phase relationship with the lead of the second variable. Both suggest a time lag between the variables of a quarter of a period length. If significant coherence and phase relationships are consistent over a certain extent of the time-frequency space, we can assume a causal relationship between the leading and the following variable (Grinsted et al. 2004; Maraun et al. 2007). In the "cone of influence," marked in a lighter shade, edge effects due to the limited length of the respective time series may distort the wavelet coherence and should be interpreted with caution. Global wavelet coherence gives an indication of the importance of scale across the entire time span, while at the same time blurring differences between time windows.

Over the course of the time span under consideration (from December 2008 until August 2009), patterns of coherence

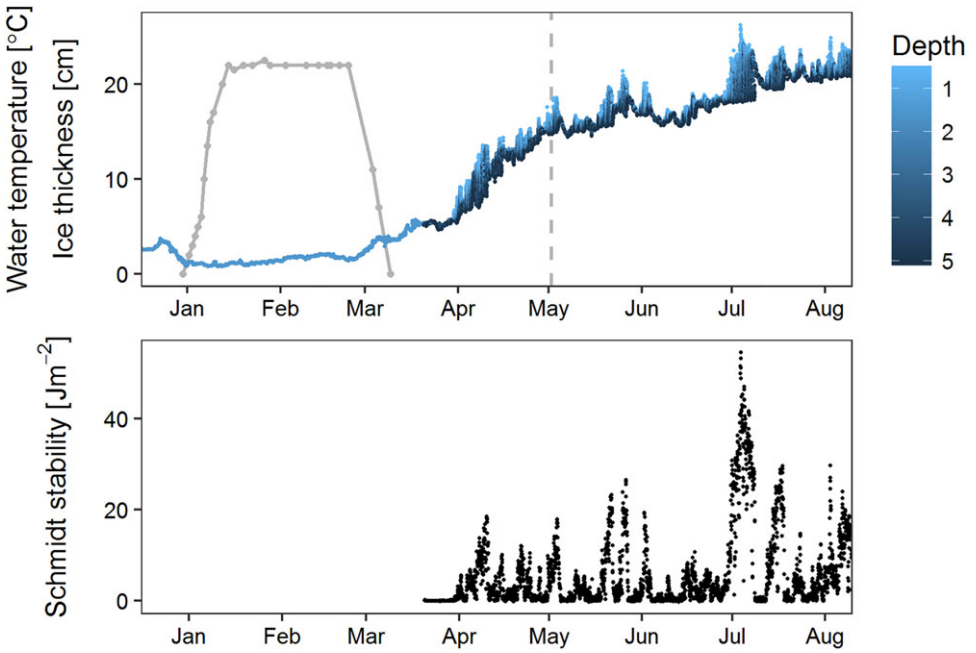

Fig. 2. Upper panel: Time series of water temperature (°C) in the Müggelsee with blue color gradient according to measurement depth; ice thickness (cm) (gray dots and line); peak of zooplankton abundance as an indicator of the clear water phase, calculated as the local maximum of the fit of a Weibull function to weekly cladocera abundance data (Rolinski et al. 2007; vertical dashed line). Bottom panel: Time series of Schmidt stability (J m^{-2}), calculated from vertical water temperature profiles.

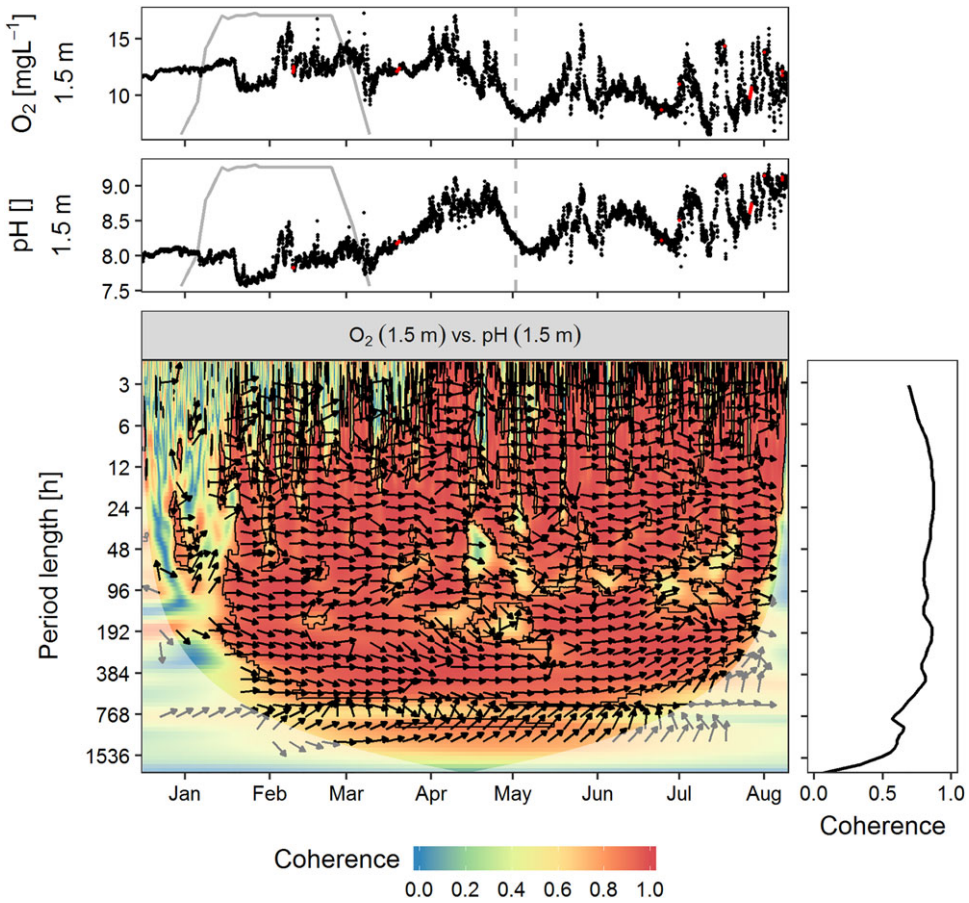

Fig. 3. Upper panels: Time series of oxygen concentration (O_2) (mg L^{-1}) and pH measured hourly at a depth of 1.5 m in the Müggelsee; time window with an ice cover (gray line); onset of the clear water phase (vertical dashed line). Bottom panel: Wavelet coherence between O_2 and pH; black contours around regions where coherence is significant against red noise, based on Monte Carlo AR1 time series (significance level 0.95) with the false discovery rate controlled at the 5% level; black arrows indicate the relative phase relationship (in-phase pointing right; antiphase pointing left; out of phase pointing up/down); the lighter shade denotes the cone of influence, where edge effects may distort patterns of coherence; period length on *y*-axis $\log_2$-transformed. Right margin panel: Global wavelet coherence, calculated as the arithmetic mean over time.

between most variables changed frequently, resulting in rather patchy patterns in Figs. 3–11. These were often restricted within the time-frequency space, and especially at short period lengths of a few hours, coherent and noncoherent phases were usually quite short lived.

Photosynthesis and respiration

High in-phase coherence between oxygen concentration and pH would indicate photosynthetic processes if both increased synchronously or respiratory processes if both decreased synchronously. We found high coherence in phase between O_2 and pH for all time scales until the end of the time span under study, except for subdaily patterns during the first month (Fig. 3). The consistently strong relationship between O_2 levels and pH was also reflected in global wavelet coherence, which was high across all time scales. Time series of oxygen concentrations and pH values showed a synchronous abrupt and substantial decline in mid-January, pointing to the dominance of respiration over photosynthesis at that time. O_2 and pH increased synchronously in early February, and even more after the thaw date, which coincided with the beginning of the spring phytoplankton bloom, indicating an increase in photosynthesis. This was followed by a substantial decrease just before the clear water phase, signaling that respiration had exceeded photosynthesis. Another 2-month cycle occurred in May and June, and several much shorter cycles occurred thereafter.

The growth of algae and cyanobacteria populations

High in-phase coherence between water temperature and levels of Chl *a* or phycocyanin would indicate growth of a phytoplankton population driven by water temperature, while high in-phase coherence between Chl *a* and phycocyanin themselves would indicate similar drivers of the dynamics of algae and cyanobacteria populations. Water temperature and Chl *a* were coherently in phase for rather brief time windows (1–3 weeks) between January and August (Fig. 4). Their strongest and longest coherence was observed during the

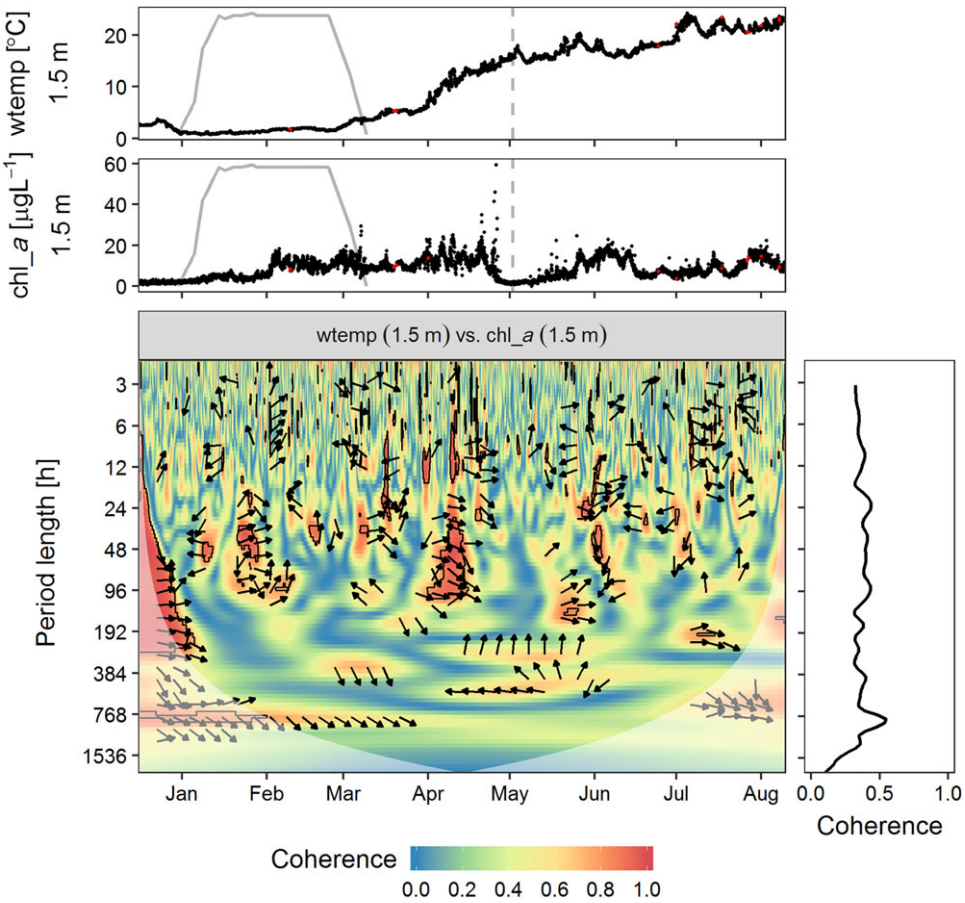

Fig. 4. Upper panels: Time series of water temperature (wtemp) (°C) and Chl *a* (µg L^{-1}) measured hourly at a depth of 1.5 m in the Müggelsee; time window with an ice cover (gray line); onset of the clear water phase (vertical dashed line). Bottom panel: Wavelet coherence between wtemp and Chl *a*; black lines, arrows and lighter shade as in Fig. 3; *y*-axis $\log_2$-transformed. Right margin panel: Global wavelet coherence, calculated as the arithmetic mean over time.

intensified spring bloom of phytoplankton in April after the thaw date; this coherence covered period lengths from a few hours up to a week. This indicates that water temperature drove the growth of phytoplankton populations during this time window. In the summer, the coherence between Chl *a* and water temperature was generally lower and more short lived, and restricted to small ranges of period lengths. This suggests that direct temperature effects did not play a major role in phytoplankton population growth in the summer. The overall global wavelet coherence was rather low, and reflected the brief nature of this relationship. It revealed a small hump at period lengths around 24 h, indicating that diurnal cycles of water temperature influenced algal development. Chl *a* and phycocyanin were coherently in phase during the first 4.5 months of 2009 for period lengths exceeding 12 h, indicating similar drivers of algae and cyanobacteria populations during this time window. This synchronicity was interrupted during the clear water phase (Fig. 5). Coherence between Chl *a* and phycocyanin was to a lesser degree re-established shortly after the clear water phase at period lengths greater than 12 h. In July, after time windows of intense and long-lasting thermal stratification as indicated by high Schmidt stabilities (Fig. 2), cyanobacteria developed a bloom that was not captured by Chl *a* fluorescence, and their coherence was low. Accordingly, global wavelet coherence between phycocyanin and Chl *a* was rather high at period lengths larger than 12 h.

Turbidity

High in-phase coherence between turbidity and either phytoplankton levels, electrical conductivity, or wind speed would indicate that either biological, chemical, or physical processes were responsible for dynamics in turbidity. The coherence between phycocyanin and turbidity was rather low and short lived most of the time (Fig. 6). Only in July, during the several weeks of the cyanobacteria bloom, was coherence high and in phase at period lengths from hours to weeks, indicating that cyanobacteria was the biological driver of turbidity during this time window. On long time scales, coherence was high during the entire time span, which was also reflected in a peak of global wavelet coherence for long time scales. Coherence between Chl *a* and turbidity exhibited largely similar patterns, due to the high coherence between Chl *a* and phycocyanin

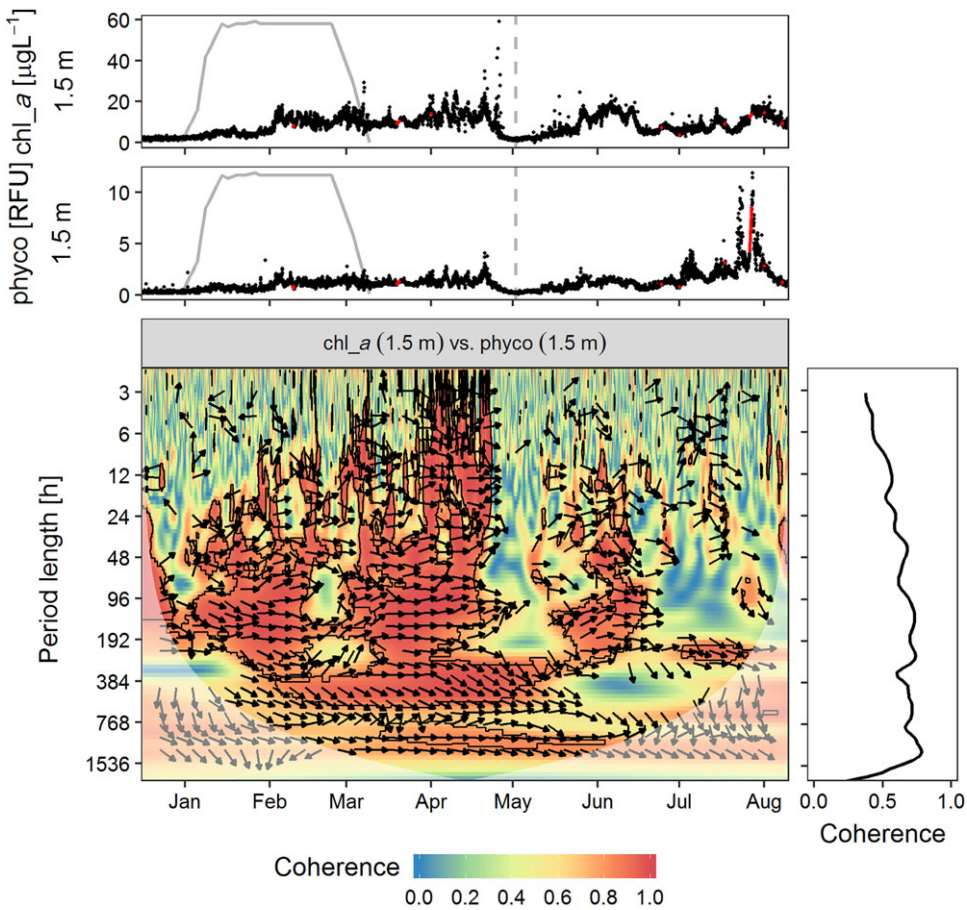

Fig. 5. Upper panels: Time series of Chl *a* (μg L^{-1}) and phycocyanin (phyco) (relative fluorescence units [RFU]) measured hourly at a depth of 1.5 m in the Müggelsee; time window with an ice cover (gray line); onset of the clear water phase (vertical dashed line). Bottom panel: Wavelet coherence between Chl *a* and phyco; black lines, arrows, and lighter shade as in Fig. 3; *y*-axis $\log_2$-transformed. Right margin panel: Global wavelet coherence, calculated as the arithmetic mean over time.

(Fig. 5), but coherence was low and short lived during the cyanobacteria bloom (not shown). One time window (in January, below the ice cover) exhibited coherent in-phase variations between electrical conductivity and turbidity at period lengths between 1 d and 1 week, indicating a chemical driver of turbidity in January (Fig. 7). Fluctuations of wind speed and turbidity were coherently in phase in May and June at scales of several days up to 2 weeks (while the weather was stormy), which was again reflected in a peak of global wavelet coherence for these time scales (Fig. 8). This indicated a physical driver of turbidity in May and June, possibly indicating the settling and resuspension of particles from the lake bottom following fluctuations in wind events.

Calcite precipitation and dissolution

High antiphase coherence between pH and electrical conductivity would indicate either calcite precipitation (if pH increased while electrical conductivity decreased) or calcite dissolution (if pH decreased while electrical conductivity increased). Coherence between pH and electrical conductivity was in an antiphase relationship during several time windows in the winter (under ice) between daily and weekly scales, during the spring bloom of phytoplankton in April on similar scales, and to a lesser extent in summer on subdaily scales (Fig. 9). The overall increase in electrical conductivity in January, accompanied by a synchronous decrease in pH, suggests calcite dissolution. In contrast, calcite precipitation was probably confined to short time windows under the ice, as the small diametrical spikes in the time series of pH and electrical conductivity indicate. Increases in pH accompanied by decreases in electrical conductivity during the spring phytoplankton bloom and during short time windows in the summer also indicated calcite precipitation. The low degree of global wavelet coherence was in agreement with the transient synchronicity between pH and electrical conductivity.

Vertical mixing

High antiphase coherence of a single variable between different measurement depths would indicate mixing of shallow and deep waters. The coherence of pH between measurements

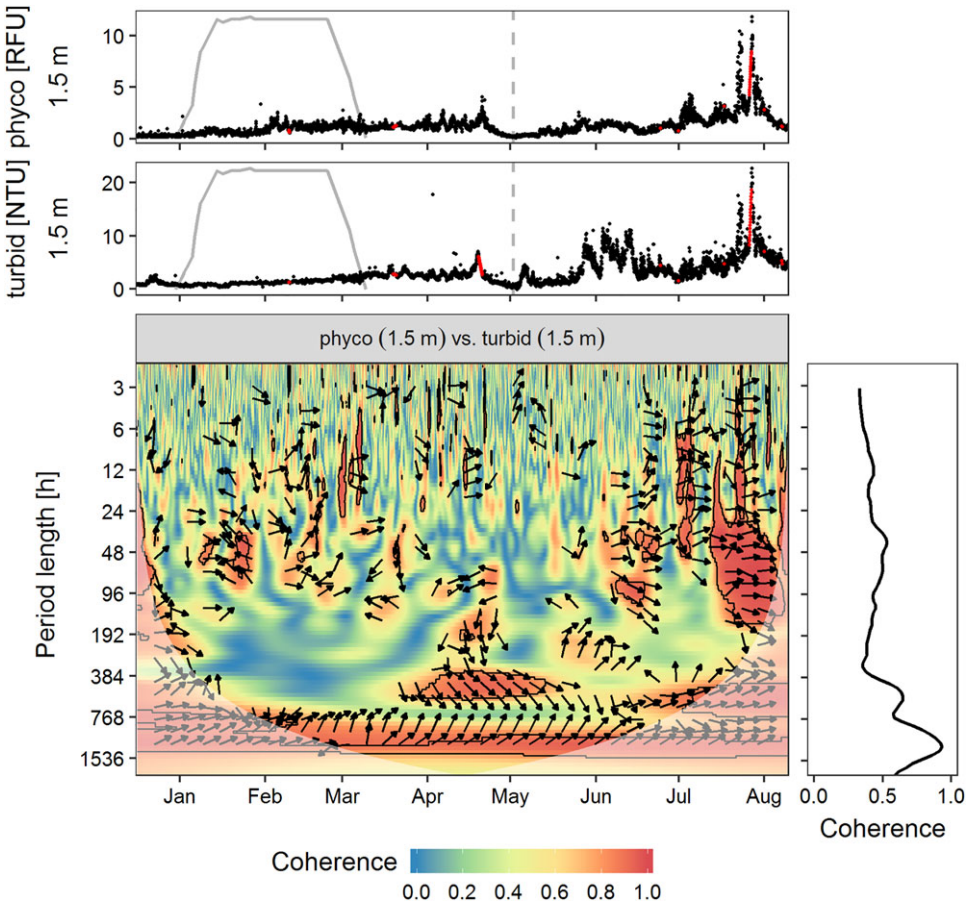

Fig. 6. Upper panels: Time series of phycocyanin (phyco) (RFU) and turbidity (turbid) (nephelometric turbidity units [NTU]) measured hourly at a depth of 1.5 m in the Müggelsee; time window with an ice cover (gray line); onset of the clear water phase (vertical dashed line). Bottom panel: Wavelet coherence between phyco and turbid; black lines, arrows, and lighter shade as in Fig. 3; *y*-axis $\log_2$-transformed. Right margin panel: Global wavelet coherence, calculated as the arithmetic mean over time.

at 1.5 and 5 m depths was high and antiphase for period lengths between 4 d and 1 week in May, and between 1 and over 2 weeks in June and July, indicating mixing between the two layers (Fig. 10). At shorter period lengths, coherence was sometimes in phase for short time windows, e.g., at period lengths around 24 h. The importance of daily and weekly time scales was also reflected in the peaks of global wavelet coherence for these time scales. Patterns of coherence for O_2 levels between the two depths in the study were very similar to those for pH (Fig. 11). Fluctuations in O_2 and pH were very large and often occurred abruptly. In particular, a steady decline toward oxygen depletion and minimum pH values in the hypolimnion during the second week of July was interrupted almost instantly, with increases of about 1.5 pH units and 10 mg L^{-1} O_2 within a few hours. Mixing events, as indicated by a Schmidt stability near zero (Fig. 2), coincided with high wind speed (Fig. 8), decreases in near-surface O_2 and pH, and increases in bottom O_2 and pH, balancing the levels of these two indicators throughout the whole water column. High coherence also was observed for other variables (water temperature, Chl *a*, phycocyanin, turbidity, and electrical conductivity), comparing measurements at depths of 1.5 and 5 m, during limited time windows and for certain period lengths (not shown). However, these results were in phase and thus could not be related to vertical mixing events.

Discussion

We have investigated in what way an analysis of automated high-frequency measurements in the time-frequency domain may help to identify and disentangle processes in a polymictic lake—the Müggelsee. Coherent dynamics among limnological and meteorological variables were detected during distinct time windows and for specific time scales. These suggested reversible processes such as photosynthesis and respiration, the growth of phytoplankton biomass, calcite precipitation and dissolution, wind-induced resuspension of sedimented particles, and vertical mixing of water masses. The following discussion examines the plausibility of attributing any synchronicity between state variables to particular processes and the characteristics of the time scales of the synchronicities identified here; this discussion is followed by an evaluation of

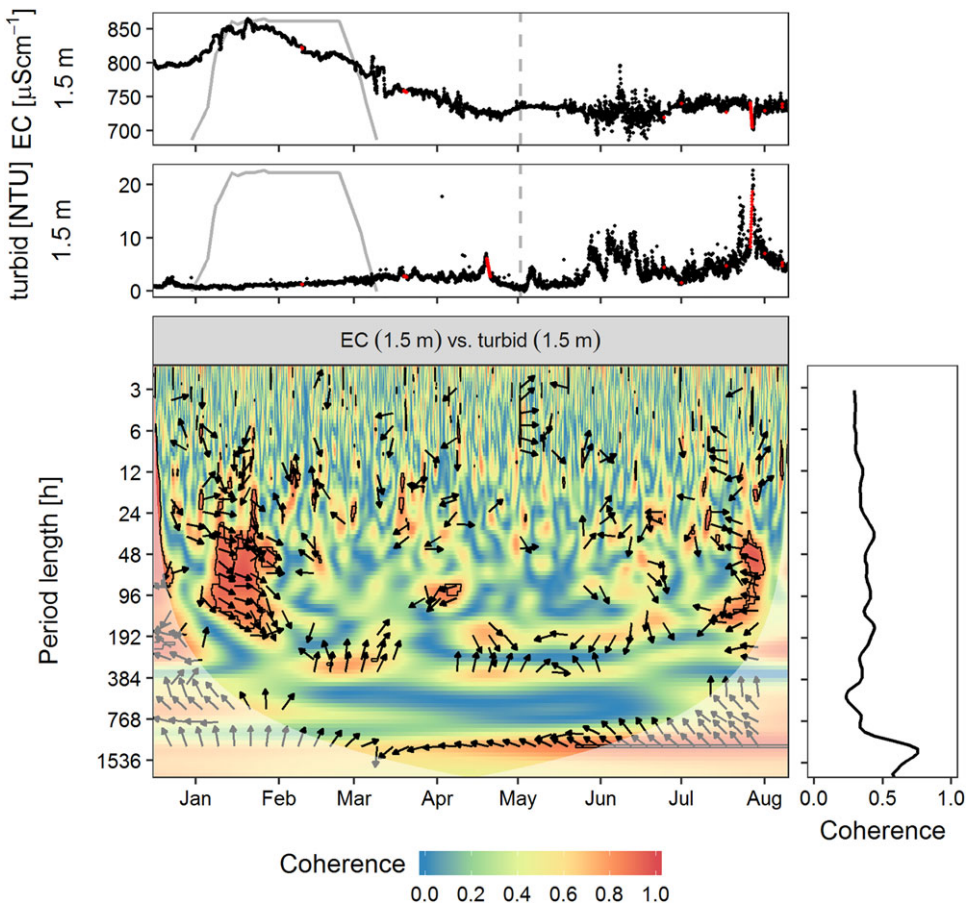

Fig. 7. Upper panels: Time series of electrical conductivity (EC) (μS cm^{-1}) and turbidity (turbid) (NTU) measured hourly at a depth of 1.5 m in the Müggelsee; time window with an ice cover (gray line); onset of the clear water phase (vertical dashed line). Bottom panel: Wavelet coherence between EC and turbid; black lines, arrows, and lighter shade as in Fig. 3; *y*-axis $\log_2$-transformed. Right margin panel: Global wavelet coherence, calculated as the arithmetic mean over time.

the methodological approach of analyzing lakes in the time-frequency domain more generally.

The plausibility of the attribution of synchronicity between variables to a given process

Under the ice cover of the Müggelsee in mid-January, we observed a synchronous decrease in O_2 and pH, which we attributed to the dominance of respiration over photosynthesis. This was substantiated by low levels of algal biomass, quantified as Chl *a* and phycocyanin, until February. Similar patterns of O_2 and pH decreases have been observed under the ice cover of several lakes and were also attributed to respiration processes (Kratz et al. 1987; Wetzel 2001; Baehr and Degrandpre 2002; Hanson et al. 2006). According to Bertilsson et al. (2013), rates of oxygen depletion and concurrent increases in the partial pressure of CO_2 are fastest after the onset of ice cover, when the ratio of photosynthesis to respiration changes in favor of respiration. The observed decrease of pH under ice can therefore be assumed to be caused by increases in pCO_2, which can lead to major undersaturation of calcite and consequential calcite dissolution (Ohlendorf and Sturm 2001). This may have led to the observed high anti-phase coherence between pH and electrical conductivity on daily to weekly scales in January, indicating calcite dissolution. It might furthermore have driven the dynamics of turbidity, as indicated by the high in-phase coherence between electrical conductivity and turbidity during the same time window and on the same time scales. Nevertheless, photosynthesis can be substantial under ice if light availability is sufficient (Wetzel 2001; Sommer et al. 2012; Hampton et al. 2017). This may account for the observed increase in O_2 and pH in February. The increase of these two indicators coincided with rising levels of Chl *a* and phycocyanin, implying that this was most likely caused by underice photosynthesis. The lack of consistent coherence between water temperature and Chl *a* below the ice indicates that the initiation of the spring phytoplankton bloom was not caused by increasing water temperatures, but probably by enhanced light conditions (Adrian et al. 1999). Oxygen concentrations and pH were coherently in phase on time scales of hours to months throughout the time window of ice cover and thereafter. The only exception was a period during the first 4 weeks of the study (in late

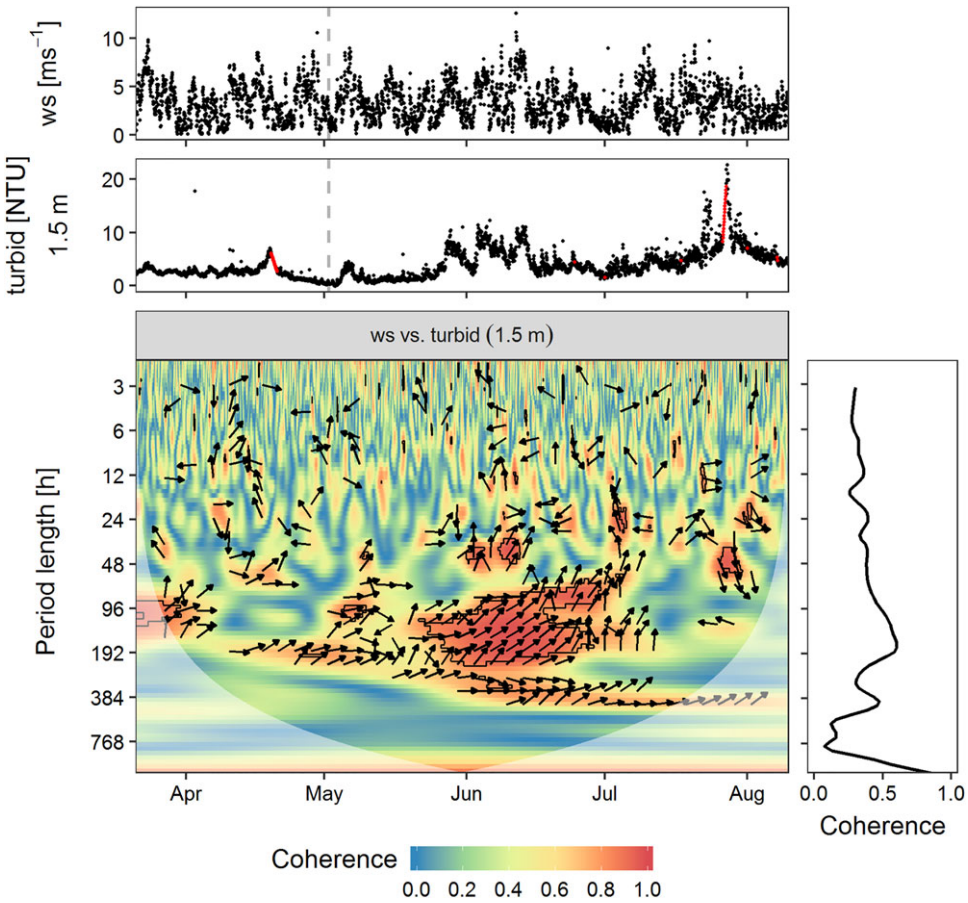

Fig. 8. Upper panels: Time series of wind speed (ws) (m s^{-1}) measured hourly at a height of 4 m above the Müggelsee and turbidity (turbid) (NTU) measured hourly at a depth of 1.5 m in the Müggelsee; time window with an ice cover (gray line); onset of the clear water phase (vertical dashed line). Bottom panel: Wavelet coherence between ws and turbid; black lines, arrows, and lighter shade as in Fig. 3; *y*-axis $\log_2$-transformed. Right margin panel: Global wavelet coherence, calculated as the arithmetic mean over time.

December and early January), when only small and non-coherent fluctuations of O_2 and pH were observed, which have to be ascribed to minor random disturbances. The high in-phase coherence of pH and O_2 between near-surface and near-bottom measurements around a period length of 24 h, revealed by global wavelet coherence, corresponds to diurnal variations in CO_2 due to metabolic day–night cycles (Morales-Pineda et al. 2014).

After ice breakup and thaw, the time window in April exhibiting the steepest increase in water temperature was the only time window showing high in-phase coherence between water temperature and Chl *a* over a broad range of time scales. In light-saturated conditions, water temperature is assumed to drive photosynthesis (Lampert and Sommer 2007). Positive results indicating the effects of spring water temperature on phytoplankton development has been shown for the Müggelsee (Gerten and Adrian 2000) and for other lakes for certain phytoplankton species (Reynolds 1990; Adrian et al. 1995; Feuchtmayr et al. 2012; Talling 2012). Li et al. (2015) found high synchronicity, estimated by wavelet coherence, between Chl *a* and water temperature in certain regions in the time-frequency space, though this was only based on monthly data. The high in-phase coherence between Chl *a* and water temperature detected during the spring bloom of phytoplankton in the Müggelsee indicated that it was only during this time window of a few weeks that water temperature and phytoplankton growth were characterized by a causal relationship. Water temperature may have driven phytoplankton growth directly by affecting replication rates, or indirectly, e.g., through control of stratification intensity, which in turn improved light availability, as deep mixing of algal cells is prevented. The high antiphase coherence between electrical conductivity and pH on daily to weekly time scales during the spring bloom of phytoplankton indicates that phytoplankton growth was accompanied by biogenic calcite precipitation during this time window. In the Müggelsee, sediment dredging has indicated the precipitation of calcite due to high photosynthetic activity (Kozerski and Kleeberg 1998). This is commonly observed in productive hard-water lakes such as the Müggelsee, where calcium is the main cation (Dudel and Kohl

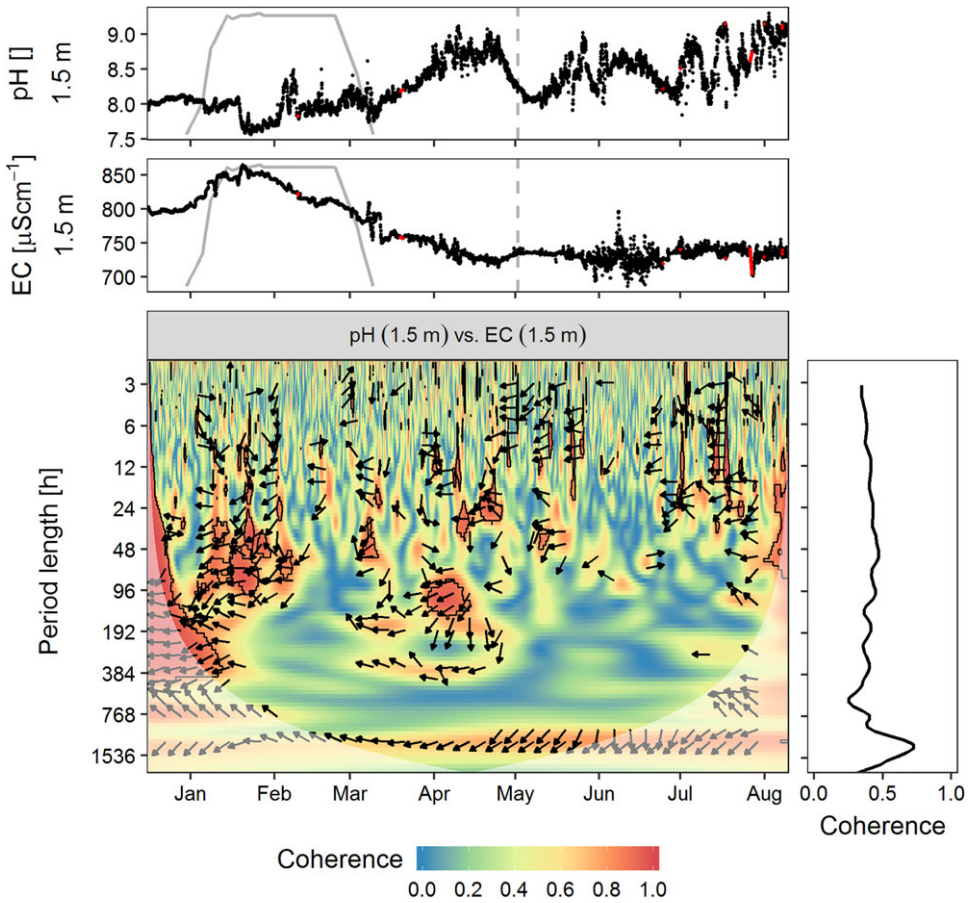

Fig. 9. Upper panels: Time series of pH and EC (μS cm^{-1}) measured hourly at a depth of 1.5 m in the Müggelsee; time window with an ice cover (gray line); onset of the clear water phase (vertical dashed line). Bottom panel: Wavelet coherence between pH and EC; black lines, arrows, and lighter shade as in Fig. 3; *y*-axis $\log_2$-transformed. Right margin panel: Global wavelet coherence, calculated as the arithmetic mean over time.

1992; Driescher et al. 1993), when photosynthetic uptake of CO_2 increases the pH, leading to oversaturation of calcite (Lampert and Sommer 2007; Heine et al. 2017). The clear water phase was characterized by the collapse of most synchronicities, most strikingly the coherence between Chl *a* and water temperature and between Chl *a* and phycocyanin, and was accompanied by substantial decreases in Chl *a*, phycocyanin, O_2 and pH. Coherences between water temperature and Chl *a* and between Chl *a* and phycocyanin were high before the clear water phase, completely absent during it, and low and briefer after it. Only the coherence between O_2 and pH remained high for all time scales, while their synchronous decrease signaled that respiration had exceeded photosynthesis. This indicates that zooplankton grazing broke the formerly synchronous relationships (Sommer et al. 2012). This has been shown to be one important explanation of the decline in spring phytoplankton blooms in the Müggelsee during the past two decades (Huber et al. 2008). The clear water phase therefore represented a crucial phenological event in the plankton development that clearly indicated a time window of altered interactions between variables and processes, and thus a change in the prevailing constraints. While a change in the prevailing constraints leading to a clear water phase is quite well known, detailed time and frequency information concerning the forces that drive it and interact within it are not. High-frequency data allows us to identify the length and time scale of those distinct time windows of interaction and the alternation of major driving forces.

After the clear water phase, the rather low and short lived coherence between water temperature and Chl *a* indicated drivers of the dynamics of the summer phytoplankton population other than water temperature, indicating a change in the prevailing constraints to phytoplankton growth. Indeed, nitrogen limitation, in contrast to water temperature, has been shown to contribute to summer phytoplankton development in the Müggelsee (Köhler et al. 2005). Cyanobacteria, on the other hand, thrive in higher water temperatures and the concomitant intense and long-lasting stratification stability (Huber et al. 2012; Merel et al. 2013), with the length of thermal stratification events rather than direct temperature effects driving cyanobacteria dominance in the Müggelsee (Wagner and Adrian 2009). As Chl *a* concentrations are inaccurate estimators of cyanobacteria

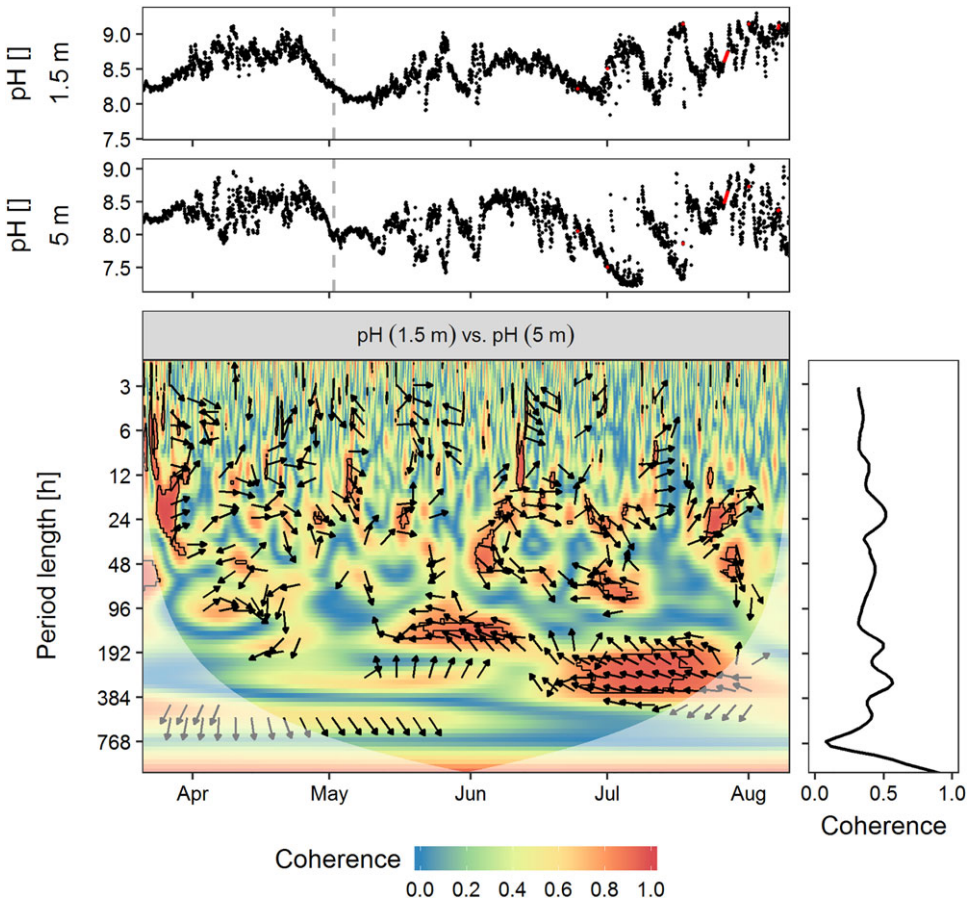

Fig. 10. Upper panels: Time series of pH measured hourly at a depth of 1.5 m and at a depth of 5 m in the Müggelsee; time window with an ice cover (gray line); onset of the clear water phase (vertical dashed line). Bottom panel: Wavelet coherence between pH measured at a depth of 1.5 m and pH measured at a depth of 5 m; black lines, arrows, and lighter shade as in Fig. 3; *y*-axis $\log_2$-transformed. Right margin panel: Global wavelet coherence, calculated as the arithmetic mean over time.

blooms (Lee et al. 1994; Brient et al. 2008), we found low coherence between Chl *a* and phycocyanin in the summer. Furthermore, cyanobacteria blooms increase the turbidity of water bodies (Paerl and Huisman 2008). This seems to be responsible for the high in-phase coherence between phycocyanin and turbidity observed during the summer bloom of cyanobacteria in the Müggelsee in July on time scales of hours to weeks. In contrast, the high in-phase coherence between turbidity and wind speed on time scales of several days to 2 weeks in June indicated wind-induced resuspension of particles. Rising wind speeds were accompanied by an increase in turbidity, indicating a resuspension of particles from the lake bottom, while calm time windows enabled these particles to settle, coinciding with low turbidity. Wind-induced resuspension is common in shallow, polymictic lakes (Kristensen et al. 1992; Kozerski and Kleeberg 1998; Eleveld 2012). Correspondingly, we found high antiphase coherence of pH and O_2 levels between near-surface and near-bottom measurements from May to July for similar time scales. This was accompanied by large synchronous diametric fluctuations of pH and O_2 in surface and bottom waters, with substantial drops in surface water oxygen concentration, while bottom waters were reoxygenated (Fig. 11). Similar patterns have been observed in other lakes and were correlated with wind events, suggesting vertical mixing (Robertson and Imberger 1994; Hanson et al. 2006; Langman et al. 2010), and in the Müggelsee from May onward in all years analyzed by Behrendt et al. (1993). The latter were related to a decoupling of production and consumption processes in surface and bottom waters, which were interrupted by irregular wind-induced changes of mixed and stratified conditions on time scales of hours to weeks (Behrendt et al. 1993). The period lengths of 4 d to 1 week in May as well as of 1 to 2 weeks in June and July, which revealed a robust antiphase coherence between near-surface and near-bottom water layers in our study, lay within the range of durations of general weather situations over Germany. These lasted 3–5 days in May, up to 8 days in June, and up to 10 days in July (Deutscher Wetterdienst, http://www.dwd.de/DE/leistungen/grosswetterlage/2009/gwl_zusammenfassung.pdf?__blob=publicationFile&v=2, last accessed 12 July 2018). As such, the attribution of high antiphase coherence between single variables measured in different

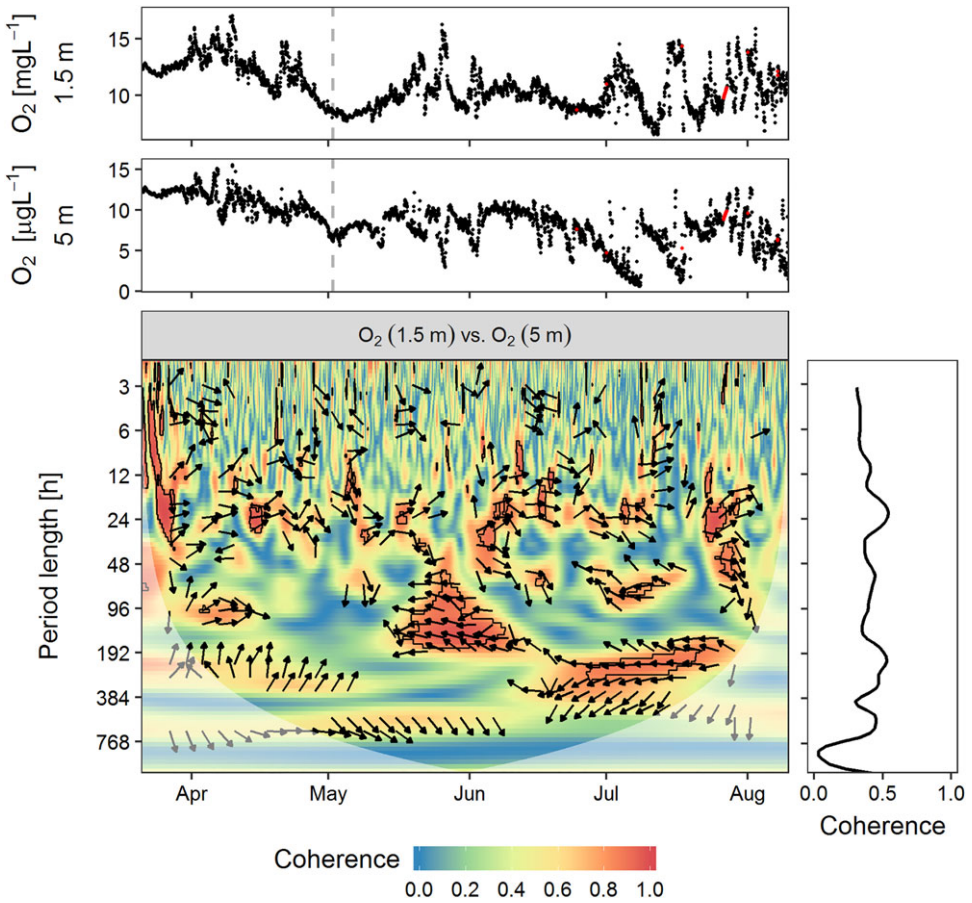

Fig. 11. Upper panels: Time series of oxygen concentration (O_2) (mg L^{-1}) measured hourly at a depth of 1.5 m and at a depth of 5 m in the Müggelsee; time window with an ice cover (gray line); onset of the clear water phase (vertical dashed line). Bottom panel: Wavelet coherence between O_2 measured at a depth of 1.5 m and O_2 measured at a depth of 5 m; black lines, arrows, and lighter shade as in Fig. 3; *y*-axis $\log_2$-transformed. Right margin panel: Global wavelet coherence, calculated as the arithmetic mean over time.

depths to vertical mixing can be substantiated, and the characteristic time scale at which vertical mixing is observed might reflect the periodicity of the general weather situation. All in all, our hypothesized relationships between patterns of coherence of various state variables and certain limnological processes proved plausible.

Measuring synchronicity—The advantages of high-resolution analysis in both the time and the frequency domain

There is a large amount of literature concerned with the temporal coherence of various state variables: Magnuson et al. (1990) and many studies thereafter (Wynne et al. 1996; Kratz et al. 1998; Rusak et al. 1999; Baines et al. 2000; Pace and Cole 2002; Chrzanowski and Grover 2005; Salmaso et al. 2014) have defined "coherence" as the synchronous dynamics of a time series of single variables among different lakes. What these studies have in common is that their measure of coherence is simple correlation analysis. They therefore lack the ability to detect transient and frequency-specific relationships, as correlations between variables may go undetected if they occur only at a certain frequency or during limited time windows. For example, Arhonditsis et al. (2004) found no correlation between water temperature and Chl *a* measured over 25 years in Lake Washington. However, their connection may have been masked by the weekly resolution of the data and the methodological approach of correlation analysis and linear regression, which lacked the ability to detect transient and potentially frequency-dependent correlations such as those revealed by our study. Other studies inferred causality from detected correlations or linear regressions between numerous state variables in lake ecosystems (Gerten and Adrian 2000; Blenckner et al. 2007; Gaiser et al. 2009; Eleveld 2012), which could have increased in accuracy and significance if a more advanced method, such as wavelet coherence, had been applied.

In this respect, the high resolution in the time and the frequency domain applied in our study has helped us to identify the respective prevailing constraints during specific time windows. For example, phytoplankton growth was related to water temperature only during short time windows (Fig. 4), pointing to other constraints or drivers of its dynamics during

the rest of the observation period. Furthermore, wavelet coherence helped to disentangle different processes that affected the same variable but to a different extent during different time windows. For example, according to our analysis, the observed dynamics of pH were related to photosynthesis and respiration (Fig. 3) for most of the study period, but also to calcite dissolution and precipitation (Fig. 9) and vertical mixing (Fig. 10) during rather short time windows. Similarly, the dynamics of turbidity were related to drivers that were biological (phycocyanin, Fig. 6), chemical (electrical conductivity, Fig. 7) as well as physical (wind speed, Fig. 8) during different time windows. Therefore, process identification cannot necessarily be derived only from the dynamics of the variables themselves, but from their joint dynamics with other variables and a time-resolved and frequency-resolved methodology. Lastly, wavelet coherence has proven its potential in identifying reversible processes that do not necessarily result in observable net effects, such as calcite dissolution observed during a rather short time window in January and reprecipitation in early April (Fig. 9). In this study, regions of high wavelet coherence in time-frequency space in most cases neither prevailed over long time windows nor covered extended time scales. This implies the difficulty of finding a generally valid level of importance for a certain time scale of coherence in abiotic and biotic interactions. This may be particularly complex in polymictic lakes, which exhibit a more immediate response to current weather conditions compared to dimictic lakes (Gerten and Adrian 2001; Benincà et al. 2011). In deeper monomictic or dimictic lakes, we would expect signals to be more consistent over scale and time. Yet, even in this lake, where we would expect processes to be briefer due to the lake's polymictic nature, we identified regions of high synchronicity, enabling the identification and disentanglement of transient processes operating in parallel.

Conclusion

Applying wavelet coherence to multivariate limnological high-frequency data proved suitable for identifying and disentangling reversible processes that affected the same variable, for detecting their characteristic time scales, and for identifying the prevailing constraints of processes that occurred during limited time windows and often in parallel. This could not have been achieved using simpler methods, such as correlation or regression analysis, as the coherence between variables was found to be frequency-specific and to depend on particular time windows. This therefore reiterates the importance of considering process-specific time scales. While a daily resolution of the data would have sufficed to identify some of the processes, such as wind-induced resuspension and vertical mixing, which took place on time scales of several days to weeks (Schmidt et al. 2018), high temporal resolution of the data was crucial for detecting characteristic time scales of variability and time windows, especially for when biological and chemical processes occurred, as both were often rather brief. Our results imply that wavelet coherence has great potential to serve as a diagnostic tool in limnology, and potentially also in other types of ecosystems but especially nonstationary ones. For example, Schaefli et al. (2007) applied wavelet coherence to a 20-yr-long time series of precipitation, temperature, and discharge in an Alpine catchment. They detected potential flood-triggering situations, while also identifying the most critical hydrometeorological constraints of different flood types.

One possible limitation of our approach is that wavelet coherence, as a statistical method, does not reveal the true underlying ecological mechanisms that cause periodicities or associations between variables (Cazelles et al. 2008). Causality can only be assumed from the phase relationship of extended regions of local cross correlation in time-frequency space. To reveal mechanisms behind coherent regions, it would be necessary to have experimental or modeling studies and more elaborate examinations of each case, possibly comprising further variables. These could, for instance, include the Granger causality (Granger 1969), or convergent cross mapping (Sugihara et al. 2012) calculated over time windows and frequency ranges where a high coherence has been identified beforehand. This may help future researchers distinguish causality from correlation, which in turn would result in higher confidence about causal mechanisms. For this reason, comparing wavelet coherence of the same set of state variables measured in different lakes over a range of mixing types, trophic states and chemical compositions would give us some insights into the general applicability of the approach and may reveal interesting connections and differences between lake types and the characteristic time scales of major processes in them. These might be promising next steps in diagnosing and understanding the processes behind temporal variability in limnological state variables.

References

Adrian, R., R. Deneke, U. Mischke, R. Stellmacher, and P. Lederer. 1995. A long-term study of the Heiligensee (1975-1992): Evidence for effects of climatic change on the dynamics of eutrophied lake ecosystems. Arch. Hydrobiol. **133**: 315–337.

Adrian, R., N. Walz, T. Hintze, S. Hoeg, and R. Rusche. 1999. Effects of ice duration on plankton succession during spring in a shallow polymictic lake. Freshw. Biol. **41**: 621–634. doi:10.1046/j.1365-2427.1999.00411.x

Adrian, R., D. Gerten, V. Huber, C. Wagner, and S. R. Schmidt. 2012. Windows of change: Temporal scale of analysis is decisive to detect ecosystem responses to climate change. Mar. Biol. **159**: 2533–2542. doi:10.1007/s00227-012-1938-1

Arhonditsis, G. B., M. Winder, M. T. Brett, and D. E. Schindler. 2004. Patterns and mechanisms of phytoplankton variability

in Lake Washington (USA). Water Res. **38**: 4013–4027. doi:10.1016/j.watres.2004.06.030

Baehr, M. M., and M. D. Degrandpre. 2002. Under-ice CO_2 and O_2 variability in a freshwater lake. Biogeochemistry **61**: 95–114. doi:10.1023/a:1020265315833

Baines, S. B., K. E. Webster, T. K. Kratz, S. R. Carpenter, and J. J. Magnuson. 2000. Synchronous behavior of temperature, calcium, and chlorophyll in lakes of northern Wisconsin. Ecology **81**: 815–825. doi:10.1890/0012-9658(2000)081[0815:SBOTCA]2.0.CO;2

Barthelmes, D. 1962. Die Bedeutung der zuflußbedingten und windbedingten Strömungen im Großen Müggelsee. Wasserwirtsch **12**: 362–365.

Behrendt, H., B. Nixdorf, and W.-G. Pagenkopf. 1993. Phenomenological description of polymixis and influence on oxygen budget and phosphorus release in Lake Müggelsee. Int. Revue. Ges. Hydrobiol. Hydrogr. **78**: 411–421. doi:10.1002/iroh.19930780310

Benincà, E., V. Dakos, E. H. Van Nes, J. Huisman, and M. Scheffer. 2011. Resonance of plankton communities with temperature fluctuations. Am. Nat. **178**: E85–E95. doi:10.1086/661902

Benjamini, Y., and D. Yekutieli. 2001. The control of the false discovery rate in multiple testing under dependency. Ann. Stat. **29**: 1165–1188. doi:10.1214/aos/1013699998

Bertilsson, S. and others 2013. The under-ice microbiome of seasonally frozen lakes. Limnol. Oceanogr. **58**: 1998–2012. doi:10.4319/lo.2013.58.6.1998

Blauw, A. N., E. Benincà, R. W. P. M. Laane, N. Greenwood, and J. Huisman. 2012. Dancing with the tides: Fluctuations of coastal phytoplankton orchestrated by different oscillatory modes of the tidal cycle. PLoS One **7**: 7. doi:10.1371/journal.pone.0049319

Blenckner, T. and others 2007. Large-scale climatic signatures in lakes across Europe: A meta-analysis. Glob. Chang. Biol. **13**: 1314–1326. doi:10.1111/j.1365-2486.2007.01364.x

Brient, L. and others 2008. A phycocyanin probe as a tool for monitoring cyanobacteria in freshwater bodies. J. Environ. Monit. **10**: 248–255. doi:10.1039/b714238b

Cazelles, B., M. Chavez, D. Berteaux, F. Ménard, J. O. Vik, S. Jenouvrier, and N. C. Stenseth. 2008. Wavelet analysis of ecological time series. Oecologia **156**: 287–304. doi:10.1007/s00442-008-0993-2

Chrzanowski, T. H., and J. P. Grover. 2005. Temporal coherence in limnological features of two southwestern reservoirs. Lake Reserv. Manag. **21**: 39–48. doi:10.1080/07438140509354411

Coble, A. A., R. G. Asch, S. Rivero-Calle, S. M. Heerhartz, J. M. Holding, C. T. Kremer, M. Finiguerra, and K. E. Strock. 2016. Climate is variable, but is our science? Limnol. Oceanogr. Bull. **25**: 71–76. doi:10.1002/lob.10115

Driescher, E., H. Behrendt, G. Schellenberger, and R. Stellmacher. 1993. Lake Müggelsee and its environment—natural conditions and anthropogenic impacts. Int. Revue. Ges. Hydrobiol. **78**: 327–343.

Dudel, G., and J.-G. Kohl. 1992. The nitrogen budget of a shallow lake (Großer Müggelsee, Berlin). Int. Revue. Ges. Hydrobiol. **77**: 43–72. doi:10.1002/iroh.19920770105

Eleveld, M. A. 2012. Wind-induced resuspension in a shallow lake from medium resolution imaging spectrometer (MERIS) full-resolution reflectances. Water Resour. Res. **48**: 1–13. doi:10.1029/2011WR011121

Feuchtmayr, H., S. J. Thackeray, I. D. Jones, M. de Ville, J. Fletcher, B. James, and J. Kelly. 2012. Spring phytoplankton phenology—are patterns and drivers of change consistent among lakes in the same climatological region? Freshw. Biol. **57**: 331–344. doi:10.1111/j.1365-2427.2011.02671.x

Gaiser, E. E., N. D. Deyrup, R. W. Bachmann, L. E. Battoe, and H. M. Swain. 2009. Effects of climate variability on transparency and thermal structure in subtropical, monomictic Lake Annie, Florida. Fundam. Appl. Limnol. **175**: 217–230. doi:10.1127/1863-9135/2009/0175-0217

Gerten, D., and R. Adrian. 2000. Climate-driven changes in spring plankton dynamics and the sensitivity of shallow polymictic lakes to the North Atlantic oscillation. Limnol. Oceanogr. **45**: 1058–1066. doi:10.4319/lo.2000.45.5.1058

Gerten, D., and R. Adrian. 2001. Differences in the persistency of the North Atlantic oscillation signal among lakes. Limnol. Oceanogr. **46**: 448–455. doi:10.4319/lo.2001.46.2.0448

Gouhier, T. C., A. Grinsted, and V. Simko. 2018. R package biwavelet: Conduct univariate and bivariate wavelet analyses (Version 0.20.17). Available from https://github.com/tgouhier/biwavelet.

Granger, C. W. J. 1969. Investigating causal relations by econometric models and cross-spectral methods. Econometrica **37**: 424–438. doi:10.2307/1912791

Grinsted, A., J. C. Moore, and S. Jevrejeva. 2004. Application of the cross wavelet transform and wavelet coherence to geophysical time series. Nonlinear Processes Geophys. **11**: 561–566. doi:10.5194/npg-11-561-2004

Guadayol, Ò., N. J. Silbiger, M. J. Donahue, and F. I. M. Thomas. 2014. Patterns in temporal variability of temperature, oxygen and pH along an environmental gradient in a coral reef. PLoS One **9**: 1–12. doi:10.1371/journal.pone.0085213

Hamilton, S. K., D. A. Bruesewitz, G. P. Horst, D. B. Weed, and O. Sarnelle. 2009. Biogenic calcite–phosphorus precipitation as a negative feedback to lake eutrophication. Can. J. Fish. Aquat. Sci. **66**: 343–350. doi:10.1139/F09-003

Hampton, S. E. and others 2017. Ecology under lake ice. Ecol. Lett. **20**: 98–111. doi:10.1111/ele.12699

Hanson, P. C., S. R. Carpenter, D. E. Armstrong, E. H. Stanley, and T. K. Kratz. 2006. Lake dissolved inorganic carbon and dissolved oxygen: Changing drivers from days to decades. Ecol. Monogr. **76**: 343–363. doi:10.1177/0888325406287176

Heine, I., A. Brauer, B. Heim, S. Itzerott, P. Kasprzak, U. Kienel, and B. Kleinschmit. 2017. Monitoring of calcite precipitation in hardwater lakes with multi-spectral remote sensing archives. Water **9**: 15. doi:10.3390/w9010015

Huber, V., R. Adrian, and D. Gerten. 2008. Phytoplankton response to climate warming modified by trophic state. Limnol. Oceanogr. **53**: 1–13. doi:10.4319/lo.2008.53.1.0001

Huber, V., C. Wagner, D. Gerten, and R. Adrian. 2012. To bloom or not to bloom: Contrasting responses of cyanobacteria to recent heat waves explained by critical thresholds of abiotic drivers. Oecologia **169**: 245–256. doi:10.1007/s00442-011-2186-7

Idso, S. B. 1973. On the concept of lake stability. Limnol. Oceanogr. **18**: 681–683. doi:10.4319/lo.1973.18.4.0681

Jennings, E. and others 2012. Effects of weather-related episodic events in lakes: An analysis based on high-frequency data. Freshw. Biol. **57**: 589–601. doi:10.1111/j.1365-2427.2011.02729.x

Kara, E. L. and others 2012. Time-scale dependence in numerical simulations: Assessment of physical, chemical, and biological predictions in a stratified lake at temporal scales of hours to months. Environ. Model. Software **35**: 104–121. doi:10.1016/j.envsoft.2012.02.014

Kasprzak, P., T. Shatwell, M. O. Gessner, T. Gonsiorczyk, G. Kirillin, G. Selmeczy, J. Padisák, and C. Engelhardt. 2017. Extreme weather event triggers cascade towards extreme turbidity in a clear-water lake. Ecosystems **20**: 1407–1420. doi:10.1007/s10021-017-0121-4

Keitt, T. H. 2008. Coherent ecological dynamics induced by large-scale disturbance. Nature **454**: 331–334. doi:10.1038/nature06935

Klug, J. L. and others 2012. Ecosystem effects of a tropical cyclone on a network of lakes in northeastern North America. Environ. Sci. Technol. **46**: 11693–11701. doi:10.1021/es302063v

Köhler, J., and B. Nixdorf. 1994. Influences of the lowland river spree on phytoplankton dynamics in the flow-through Lake Müggelsee (Germany). Hydrobiologia **275**: 187–195. doi:10.1007/BF00026710

Köhler, J., S. Hilt, R. Adrian, A. Nicklisch, H. P. Kozerski, and N. Walz. 2005. Long-term response of a shallow, moderately flushed lake to reduced external phosphorus and nitrogen loading. Freshw. Biol. **50**: 1639–1650. doi:10.1111/j.1365-2427.2005.01430.x

Kozerski, H.-P., and A. Kleeberg. 1998. The sediments and benthic-pelagic exchange in the shallow lake Müggelsee (Berlin, Germany). Int. Rev. Hydrobiol. **83**: 77–112. doi:10.1002/iroh.19980830109

Kratz, T. K., R. B. Cook, C. J. Bowser, and P. L. Brezonik. 1987. Winter and spring pH depressions in northern Wisconsin lakes caused by increases in pCO_2. Can. J. Fish. Aquat. Sci. **44**: 1082–1088. doi:10.1139/f87-129

Kratz, T. K., P. A. Soranno, S. B. Baines, B. J. Benson, J. J. Magnuson, T. M. Frost, and R. C. Lathrop. 1998. Interannual synchronous dynamics in north temperate lakes in Wisconsin, USA, p. 273–287. *In* D.G. George, J.G. Jones, C.S. Puncochar, C.S. Reynolds, and D.W. Sutcliffe [ed.], Management of lakes and reservoirs during global climate change. Kluwer Academic Publishers.

Kristensen, P., M. Søndergaard, and E. Jeppesen. 1992. Resuspension in a shallow eutrophic lake. Hydrobiologia **228**: 101–109. doi:10.1007/BF00006481

Lampert, W., and U. Sommer. 2007. Limnoecology: The ecology of lakes and streams, 2nd ed. Oxford Univ. Press.

Langman, O. C., P. C. Hanson, S. R. Carpenter, and Y. H. Hu. 2010. Control of dissolved oxygen in northern temperate lakes over scales ranging from minutes to days. Aquat. Biol. **9**: 193–202. doi:10.3354/ab00249

Lee, T., M. Tsuzuki, T. Takeuchi, K. Yokoyama, and I. Karube. 1994. In vivo fluorometric method for early detection of cyanobacterial waterblooms. J. Appl. Phycol. **6**: 489–495. doi:10.1007/BF02182403

Li, W., B. Qin, and Y. Zhang. 2015. Multi-temporal scale characteristics of algae biomass and selected environmental parameters based on wavelet analysis in Lake Taihu, China. Hydrobiologia **747**: 189–199. doi:10.1007/s10750-014-2135-7

Magnuson, J. J., B. J. Benson, and T. K. Kratz. 1990. Temporal coherence in the limonology of a suite of lakes in Wisconsin, U.S.A. Freshw. Biol. **23**: 145–149. doi:10.1111/j.1365-2427.1990.tb00259.x

Maraun, D., and J. Kurths. 2004. Cross wavelet analysis: Significance testing and pitfalls. Nonlinear Processes Geophys. **11**: 505–514. doi:10.5194/npg-11-505-2004

Maraun, D., J. Kurths, and M. Holschneider. 2007. Nonstationary Gaussian processes in wavelet domain: Synthesis, estimation, and significance testing. Phys. Rev. E Stat. Nonlinear Soft Matter Phys. **75**: 1–14. doi:10.1103/PhysRevE.75.016707

Marcé, R. and others 2016. Automatic high frequency monitoring for improved lake and reservoir management. Environ. Sci. Technol. **50**: 10780–10794. doi:10.1021/acs.est.6b01604

Meinson, P., A. Idrizaj, P. Nõges, T. Nõges, and A. Laas. 2016. Continuous and high-frequency measurements in limnology: History, applications, and future challenges. Environ. Rev. **24**: 52–62. doi:10.1139/er-2015-0030

Merel, S., D. Walker, R. Chicana, S. Snyder, E. Baurès, and O. Thomas. 2013. State of knowledge and concerns on cyanobacterial blooms and cyanotoxins. Environ. Int. **59**: 303–327. doi:10.1016/j.envint.2013.06.013

Morales-Pineda, M., A. Cózar, I. Laiz, B. Úbeda, and J. A. Gálvez. 2014. Daily, biweekly, and seasonal temporal scales of pCO_2 variability in two stratified Mediterranean reservoirs. J. Geophys. Res. Biogeo. **119**: 509–520. doi:10.1002/2013JG002317

Ohlendorf, C., and M. Sturm. 2001. Precipitation and dissolution of calcite in a Swiss high alpine lake. Arctic. Antarct. Alp. Res. **33**: 410–417. doi:10.2307/1552550

Pace, M. L., and J. J. Cole. 2002. Synchronous variation of dissolved organic carbon and color in lakes. Limnol. Oceanogr. **47**: 333–342. doi:10.4319/lo.2002.47.2.0333

Paerl, H. W., and J. Huisman. 2008. Blooms like it hot. Science **320**: 57–58. doi:10.1126/science.1155398

R Core Team. 2018. R: A language and environment for statistical computing. R Foundation for Statistical Computing. Available from https://www.R-project.org/.

Read, J. S., D. P. Hamilton, I. D. Jones, K. Muraoka, L. Winslow, R. Kroiss, C. H. Wu, and E. Gaiser. 2011. Derivation of lake mixing and stratification indices from high-resolution lake buoy data. Environ. Model. Software **26**: 1325–1336. doi:10.1016/j.envsoft.2011.05.006

Reynolds, C. S. 1990. Temporal scales of variability in pelagic environments and the response of phytoplankton. Freshw. Biol. **23**: 25–53. doi:10.1111/j.1365-2427.1990.tb00252.x

Robertson, D. M., and J. Imberger. 1994. Lake number, a qualitative indicator of mixing used to estimate changes in dissolved oxygen. Int. Rev. ges. Hydrobiol. **79**: 159–176. doi: 10.1002/iroh.19940790202

Rolinski, S., H. Horn, T. Petzoldt, and L. Paul. 2007. Identifying cardinal dates in phytoplankton time series to enable the analysis of long-term trends. Oecologia **153**: 997–1008. doi:10.1007/s00442-007-0783-2

Rusak, J. A., N. D. Yan, K. M. Somers, and D. J. McQueen. 1999. The temporal coherence of zooplankton population abundances in neighboring north-temperate lakes. Am. Nat. **153**: 46–58. doi:10.1086/303147

Salmaso, N., F. Buzzi, L. Cerasino, L. Garibaldi, B. Leoni, G. Morabito, M. Rogora, and M. Simona. 2014. Influence of atmospheric modes of variability on the limnological characteristics of large lakes south of the Alps: A new emerging paradigm. Hydrobiologia **731**: 31–48. doi:10.1007/s10750-013-1659-6

Schaefli, B., D. Maraun, and M. Holschneider. 2007. What drives high flow events in the Swiss Alps? Recent developments in wavelet spectral analysis and their application to hydrology. Adv. Water Resour. **30**: 2511–2525. doi:10.1016/j.advwatres.2007.06.004

Schmidt, S. R., D. Gerten, T. Hintze, G. Lischeid, D. M. Livingstone, and R. Adrian. 2018. Temporal and spatial scales of water temperature variability as an indicator for mixing in a polymictic lake. Inl. Waters **8**: 82–95. doi: 10.1080/20442041.2018.1429067

Schmidt, W. 1928. Über Temperatur- und Stabilitätsverhaltnisse von seen. Geogr. Ann. **10**: 145–177.

Sommer, U., Z. M. Gliwicz, W. Lampert, and A. Duncan. 1986. The PEG-model of seasonal succession of planktonic events in fresh waters. Arch. Hydrobiol. **106**: 433–471.

Sommer, U. and others 2012. Beyond the plankton ecology group (PEG) model: Mechanisms driving plankton succession. Annu. Rev. Ecol. Evol. Syst. **43**: 429–448. doi:10.1146/annurev-ecolsys-110411-160251

Sugihara, G., R. May, H. Ye, C. Hsieh, E. Deyle, M. Fogarty, and S. Munch. 2012. Detecting causality in complex ecosystems. Science **338**: 496–500. doi:10.1126/science.1227079

Talling, J. F. 2012. Temperature increase - an uncertain stimulant of algal growth and primary production in fresh waters. Freshw. Rev. **5**: 73–84. doi:10.1608/FRJ-5.2.471

Torrence, C., and G. P. Compo. 1998. A practical guide to wavelet analysis. Bull. Am. Meteorol. Soc. **79**: 61–78. doi: 10.1175/1520-0477(1998)079<0061:APGTWA>2.0.CO;2

Vargas, R., M. Detto, D. D. Baldocchi, and M. F. Allen. 2010. Multiscale analysis of temporal variability of soil CO_2 production as influenced by weather and vegetation. Glob. Chang. Biol. **16**: 1589–1605. doi:10.1111/j.1365-2486.2009.02111.x

Vasseur, D. A. and others 2014. Synchronous dynamics of zooplankton competitors prevail in temperate lake ecosystems. Proc. R. Soc. B Biol. Sci. **281**: 20140633. doi:10.1098/rspb.2014.0633

Wagner, C., and R. Adrian. 2009. Cyanobacteria dominance: Quantifying the effects of climate change. Limnol. Oceanogr. **54**: 2460–2468. doi:10.4319/lo.2009.54.6_part_2.2460

Wetzel, R. G. 2001. Limnology, 3rd ed. Academic Press.

Wickham, H. 2009. ggplot2: Elegant graphics for data analysis. Springer-Verlag, Available from http://ggplot2.org.

Wilhelm, S., and R. Adrian. 2008. Impact of summer warming on the thermal characteristics of a polymictic lake and consequences for oxygen, nutrients and phytoplankton. Freshw. Biol. **53**: 226–237. doi:10.1111/j.1365-2427.2007.01887.x

Winslow, L., J. Read, R. Woolway, J. Brentrup, T. Leach, and J. Zwart. 2016. rLakeAnalyzer: Lake physics tools. R package version 13. Available from https://cran.r-project.org/package=rLakeAnalyzer.

Wynne, R. H., J. J. Magnuson, M. K. Clayton, T. M. Lillesand, and D. C. Rodman. 1996. Determinants of temporal coherence in the satellite-derived 1987-1994 ice breakup dates of lakes on the Laurentian shield. Limnol. Oceanogr. **41**: 832–838. doi:10.4319/lo.1996.41.5.0832

Acknowledgments

This project was funded by the DFG's LakeRisk Project (AD 91/13-1). Silke R. Schmidt was additionally supported by scholarships from the Potsdam Graduate School and from the Office of Equal Opportunity and Diversity of the University of Potsdam. This work profited from her participation in the Global Lake Ecological Observatory Network (GLEON). Rita Adrian was jointly supported by the French Foundation for Research on Biodiversity (FRB) through its synthesis center, CESAB (http://www.cesab.org/), and the John Wesley Powell Center for Analysis and Synthesis (https://powellcenter.usgs.gov/), and the MANTEL project (H2020-MSCA-ITN-2016). The authors are grateful to Dieter Gerten, Ulrike Scharfenberger, Torsten Seltmann, Benjamin Kraemer, Tom Shatwell, and Daniel Langenhaun for fruitful discussions and to two anonymous reviewers for their valuable comments.

Conflict of Interest

None declared.

Submitted 19 July 2017
Revised 13 July 2018
Accepted 28 August 2018

Editor: Robert Howarth